Bull. Chem. Soc. Ethiop. **2025**, 39(4), 749-761.
DOI: https://dx.doi.org/10.4314/bcse.v39i4.11

ISSN 1011-3924
Printed in Ethiopia
Online ISSN 1726-801X

# ENHANCE FOOD SECURITY: SUSTAINED RELEASE OF CLOVE ESSENTIAL OIL MICROCAPSULES

Haochen Wu, Tao Jiang, Xiaohong Chen and Ping Liu*

School of Materials and Chemistry, University of Shanghai for Science and Technology, Shanghai, China

(Received August 27, 2024; Revised December 28, 2024; Accepted December 30, 2024)

**ABSTRACT**. Foodborne illnesses remain a significant concern in the realm of public health. Managing food spoilage and controlling pathogenic microorganisms rely on synthetic chemicals, regrettably accompanied by various unfavourable attributes. In response to the escalating demand for innovative and secure alternative approaches, there has been a surge in the investigation of naturally sourced agents possessing antimicrobial characteristics, among which essential oils stand out. This study focuses on improving the stability of clove essential oil (CEO), and to achieve controlled release, the CEO microcapsules are prepared by solvent evaporation method with ethyl cellulose as the wall material. The results indicated optimum technological conditions: wall material mass fraction of 3%, core wall ratio of 1.0:1.5, emulsifier mass fraction of 8% and shear rate of 14000 r/min. Under these conditions, the encapsulation efficiency is 81.28%, and the yield rate is 90.58%. The CEOM were spherical with a size of 1.43-3.92 μm and had good thermal stability. The microcapsule under 50% ethanol showed a faster release rate and significant release amount. The microencapsulation of CEO with ethyl cellulose can not only improve the stability of CEO but also realise the controlled release of CEO, which has tremendous application value in antibacterial packaging.

**KEY WORDS:** Clove essential oil, Ethyl cellulose, Solvent evaporation method, Orthogonal array, Sustained release

## INTRODUCTION

Plant essential oils (EOs) are derived from various plant parts such as roots, stems, leaves and flowers. These EOs are rich in compounds like aldehydes, phenols, terpenes and alcohols, all possessing extensive antifungal capabilities. Notably, they exhibit broad-spectrum antifungal properties and are susceptible to natural biodegradation. Consequently, these EOs have found extensive utilization in food preservation [1]. Up to now, various types of EOs have been employed to hinder the proliferation of mould. In a study conducted by Arasu *et al.* [2], it was observed that Garlic EO demonstrated notable efficacy in suppressing the growth of *A. flavus* and *A. niger* on plum surfaces. Moreover, Reyes-Jurado *et al.* [3] found that thyme EO exhibited significant potential in preventing the development of mould contaminants on corn tortillas. Additionally, Achar *et al.* [4] demonstrated the eradication of *A. flavus* from peanut seeds using different concentrations of clove (500 ppm), thyme (1000 ppm), and cinnamon (2000 ppm) EOs. Besides, Pandey *et al.* [5] found that clove EO nanoemulsion coating can extend the apple piece's storage time to 10–12 days at a lower temperature.

While EOs exhibit notable antifungal properties, their significant volatility presents a challenge when considering their utilisation in grain storage and food preservation. As a result, there has been a growing research focus on finding ways to prolong the volatilisation process of EOs. Various studies have demonstrated that encapsulating EOs can effectively retard the volatilisation rate, decrease the depletion of active constituents, enhance antifungal stability, and simplify their handling, transportation, and preservation [6]. Jiang *et al.* [7] prepared lavender EO microcapsule, which has a long-acting toxic effect on Sitophilus granaries. Zhang *et al.* [8]

*Corresponding authors. E-mail: liuping_usst@outlook.com

synthesized star anise EO encapsulated by depolymerized pectin and rice protein. Results show that it has an antibacterial effect on crab meatballs inoculated with *E. coli*. Wang *et al.* [9] prepared polylactic acid bilayer films containing CEO, and the results demonstrated that films with varying CEO distributions exhibited different levels of antibacterial activity. Milagres de Almeida et al. [10] unveiled that the clove essential oil microcapsules (CEOM) has strong antimicrobial effects when not synergistic with other EOs. Considering the benefits of encapsulated EOs, the research on improving EO microcapsule storage time holds significant value and exhibits promising potential.

As for the preparation techniques of microcapsules, which include complex condensation, solvent evaporation, spray drying, solution polymerization, etc. [11-13]. The solvent evaporation technique involves dispersing both the wall material and core material within the emulsion system in the form of minute droplets. Owing to their varying degrees of hydrophobicity, a phase separation occurs when the solvent, characterized by its low boiling point, is eliminated via heating and stirring. The wall material, possessing lower hydrophobic characteristics, tends to selectively move towards the water-oil interface, where it assembles to create the capsule wall [14]. This procedure compares other techniques, does not entail any chemical reactions and offers a straightforward preparation process under mild conditions, making it conducive to achieving production feasibility on a scale [15].

This work aimed to optimise better parameters of clove essential oil (CEO) embedded in ethyl cellulose by calculating encapsulation efficiency and yield rate. Besides, the release rate of CEOM in different mediums was investigated. The findings of this research will provide a theoretical basis for plant EO microcapsule as a natural Bactericidal ingredient agent used for application value in food storage and processing.

## EXPERIMENTAL

### *Materials*

CEO was purchased from Shanghai Aladdin Biochemical Technology Co., Ltd (Shanghai, China) and stored at 4℃ for later use. Ethyl cellulose and Tween 80 were purchased from Shanghai Maclin Biochemical Technology Co., Ltd (Shanghai, China). Dichloromethane, anhydrous ethanol, potassium bromide and acetic acid were purchased from Tianjin Fuyu Fine Chemical Co., Ltd (Tianjin, China). Deionized water was prepared in the laboratory.

### *Synthesis and Characterization of CEOM*

#### *Synthesis of CEOM*

CEO was encapsulated into ethyl cellulose (wall material) with Tween 80 as emulsifier via solvent evaporation. CEOM were prepared under the following steps: (1) Prepare aqueous phase: Dissolving Tween-80 in deionized water. (2) Prepare oleic phase: Add clove essential oil to 25% of the dichloromethane solution of ethyl cellulose and stir it until completely dissolved. (3) Solution mixture: Gradually added oil phase to water phase under agitation. After that, the solution was placed under high-speed shearing for 15 minutes until entirely emulsified. (4) Postprocessing: The microcapsule suspension was obtained by agitating the mixture solution at room temperature to eliminate the dichloromethane. Following this, CEOM was acquired through freeze-drying after centrifugation and washing processes.

#### *Fourier transform infrared spectroscopy*

In order to prove that the CEO has succeeded in encapsulating in ethyl cellulose, take CEO, ethyl cellulose and CEOM respectively mixed with potassium bromide (sample: potassium bromide =

1:150). After that, samples were tested by Fourier transform infrared spectroscopy (FTIR, Thermo Fisher Scientific Inc., USA). Recorded spectra from 4000 to 400 $cm^{-1}$ and the resolution is 2 $cm^{-1}$.

*Particle characterization*

The particle size of dried CEOM was determined by the Mastersizer 2000 laser particle size analyser (Malvern Panalytical, United Kingdom), and the volume percentage of samples in different intervals in the range of 0.02-2000 μm was obtained. After 90 days, analyses again to observe size changes.

*Scanning electron microscope*

In order to analyse CEMO microstructural and longtime storage stability, the microcapsule specimens were affixed directly to the conductive adhesive to undergo gold spray treatment, and their structure was examined using a scanning electron microscope (SEM, FEI, USA), with an acceleration voltage set at 5 keV.

*Thermogravimetric analysis*

To establish the protective qualities of the wall material for the CEO, we conducted thermogravimetric analysis (TGA) involving CEO, ethyl cellulose, and CEOM using a thermogravimetric analyser (TA Instruments, USA) in a nitrogen environment. The testing process heating the samples from room temperature to 550 ℃ at a rate of 10 ℃ per minute.

*Single factor experiment and orthogonal array testing technique*

*Single factor experiment optimisation*

The amount of dichloromethane and shear time were controlled unchanged. The effect of material (1%, 2%, 3%, 4% and 5%), core wall ratio (1.1:1.0, 1.1:1.25, 1.1:1.50, 1.1:1.75, 1.1:2.0), mass fraction of emulsifier (2%, 4%, 6%, 8%, 10%) and shear rates (10000, 12000, 14000, 16000 and 18000 r/min) in encapsulation efficiency and yield rate were studied by single factor experiment (SFE) respectively. One factor was changed, while the other factor was kept constant at a time.

*Optimisation of orthogonal array testing technique*

Based on SFE, the two worst values on both ends were removed to simplify the number of orthogonal tests. The L9($3^4$) orthogonal array testing technique (OATS) table was applied, taking encapsulation efficiency and yield rate as indicators. The details of factors and levels are shown in Table 1.

Table 1. Factors and their levels for CEOM preparation.

| Factors | Symbols | Levels | | |
|---|---|---|---|---|
| | | 1 | 2 | 3 |
| Wall material (wt%) | A | 2 | 3 | 4 |
| Core wall ratio | B | 1.0:1.25 | 1.0:1.50 | 1.0:1.75 |
| Emulsifier (wt%) | C | 4 | 6 | 8 |
| Shear rates (r/min) | D | 12000 | 14000 | 16000 |

*Determination method of encapsulation efficiency and yield rate*

*Establish the standard curve of CEO*

Prepared CEO-anhydrous ethanol solution for 0.01 mg/mL, 0.02 mg/mL, 0.03 mg/mL, 0.04 mg/mL, 0.05 mg/mL and 0.06 mg/mL respectively[16]. Draw the standard curve of CEO by ultraviolet–visible (UV-Vis) spectrophotometer (Thermo Fisher, USA), which is equipped with a 1.00 cm quartz cell at room temperature (25 °C). The spectral bandwidth is 1 nm, the integration time 0.03 s, and the scan speed 1200 nm $min^{-1}$. The spectra were recorded over the wavelength 282 nm, according to Ghavidel *et al.* [17].

*Calculate the encapsulation efficiency and yield rate*

In order to measure the encapsulate effect, the encapsulation efficiency (E) and yield rate (Y) were calculated using equations (1) and (2), respectively, based on the methodology proposed by Milagres de Almeida *et al.* [18].

$$E(\%)=\frac{\text{Weight of embedded CEO}}{\text{Initial CEO weight}}\times 100\% \quad (1)$$

$$Y(\%)=\frac{\text{Total weight of CEOM}}{\text{Initial CEO weight + Initial ethyl cellulose weight}}\times 100\% \quad (2)$$

CEOM weighing 10 mg was dissolved in 10 mL of anhydrous ethanol and subjected to ultrasound for 20 min at ambient temperature to break wall material. Following filtration, the resulting filtrate underwent treatment with anhydrous ethanol, and its absorbance at 282 nm was subsequently assessed. Finally, use the CEO standard curve to calculate the weight of embedded CEO in microcapsules.

*Sustained release performance of CEOM*

In order to investigate CEOM package stability when food is warm, in vitro release behavior of CEOM was simulated with four mediums: water, alcohol (10% ethanol), oiliness (50% glycerin) and acidity (3% acetic acid) [19]. Placed 20 mg of CEO and CEOM inside a dialysis bag filled with 5 mL of the release medium, respectively. Sealed this dialysis bag within a centrifugal tube containing 25 mL of the release medium. Subsequently, set up an oscillation at both 25 ℃ and 37 ℃. During oscillation, extract 2 mL of the release medium at various intervals and got its absorbance at 282 nm. After extract, replenished an equivalent volume of the release medium into the centrifugal tube. The cumulative release amount (W) was calculated according to equation (3).

$$W(\%)=\frac{(C_t+\frac{v}{V}\sum_0^t C_t)\times V}{m}\times 100\% \quad (3)$$

wherein $C_t$ is the mass concentration of clove essential oil measured at time t, v is the volume of release medium taken out each time (2 mL), V is the total volume of liquid in the centrifugal tube (30 mL), and m is the initial mass of microcapsules in the dialysis bag (20 mg), respectively.

*Statistical analysis*

The experiments were carried out in triplicate, and the results were calculated by Duncan's multiple range test and the mean values ± standard deviations. Herein, $p > 0.05$ indicated that insignificant difference, while $p < 0.01$ indicated extremely significant difference. Data processing and graphical representation of the experimental data were performed using Excel 2021, Origin 2022, and SPSS 20.0.

## RESULTS AND DISCUSSION

### *Characterisation of CEOM*

#### *Standard curve of CEO*

A calibration curve was drawn to exhibit the relationship between the concentration of CEO and the absorbance at 282 nm ($y = 23.397x + 0.0218$, $R^2 = 0.9973$, Figure 1).

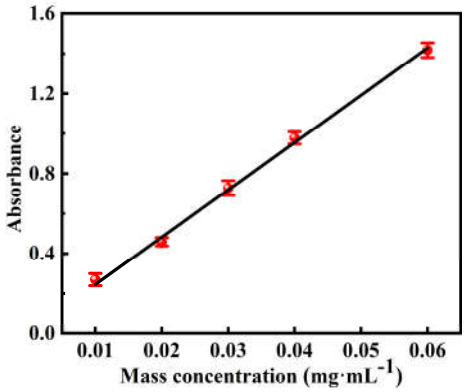


Figure 1. Standard curve of CEO at 282 nm.

#### *FTIR spectra*

Based on the infrared spectrum, the CEO's C-C bond stretching vibration peak manifested at 2910, 1514, and 1272 $cm^{-1}$, respectively, while the stretching vibration peak of the phenolic hydroxyl group was observed within the 3180-2610 $cm^{-1}$ range. The -OH bond stretching vibration peak of ethyl cellulose emerged between 3550-3345 $cm^{-1}$, and the $-CH_2$ bond stretching vibration peak was noted at 2975 $cm^{-1}$, with a bending vibration peak at 1483 $cm^{-1}$ [20, 21]. The $-CH_3$ bond bending vibration peak was also evidenced at 1379 $cm^{-1}$ [20]. These distinctive peaks were detected in the spectrogram of CEOM (Figure 2), signifying the successful encapsulation of CEO within ethyl cellulose to produce CEOM.

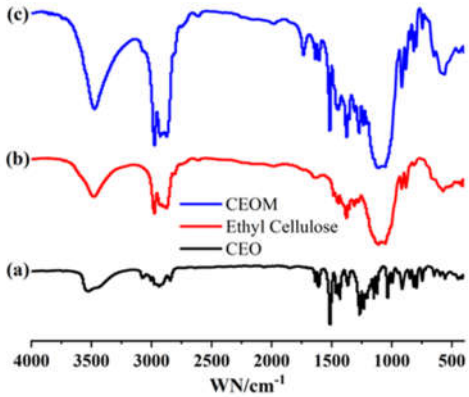


Figure 2. Infrared spectra for (a) CEO, (b) Ethyl Cellulose and (c) CEOM, respectively.

*Size of particles*

As shown in Figure 3, the CEOM exhibited an average particle size of 12.40 μm with a polydispersity index of 0.814, indicating a relatively uniform size distribution. Subsequent assessment following a 90 days storage period at room temperature revealed a slight increase in the average particle size to 12.56 μm and a marginal rise in the polydispersity index to 0.822. This change behavior suggests that the size of CEOM remained reasonably constant over the 90 days at room temperature, demonstrating notable stability.

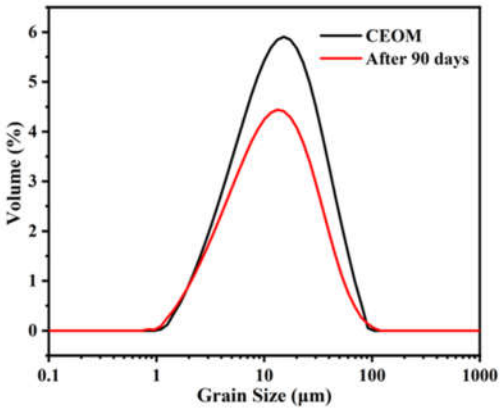


Figure 3. The particle size distribution of CEOM after preparation and 90 days of storage.

*Microstructural analysis*

The microcapsule's morphology and configuration are shown in Figure 4a. The image illustrates a spherical shape without evident fractures or voids on the capsule wall, showcasing a well-preserved structure with uniform dispersion and an absence of notable clumping. These findings suggest superior quality for CEOM prepared under optimized conditions. In order to assess CEOM stability over time, the CEOM were stored at room temperature for 90 days and then examined using SEM. Figure 4b demonstrates that the CEOM retained their spherical shape even after this extended storage period, maintaining a relatively unchanged structure. SEM images indicate that the morphology of the produced CEOM remained stable without significant alterations following prolonged storage.

*Thermogravimetric analysis*

Figure 5 demonstrates the TGA profiles of CEO, ethyl cellulose and CEOM. The data illustrates the vulnerability of the CEO to elevated temperatures, evident by its weight loss onset at 75 ℃ and a significant 75% reduction at 180 ℃. However, subsequent microcapsule preparation bolstered the oil's stability under high temperatures. The weight loss initiation was delayed to 125 ℃, with an 80% decrease at 370 ℃. These results underscore the role of ethyl cellulose as a protective barrier, enhancing the stability of CEOM.

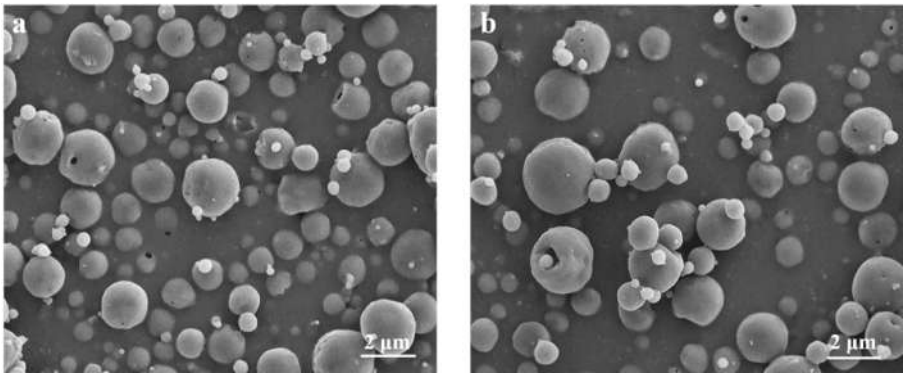


Figure 4. Microstructural analysis of CEOM. SEM images for the CEOM after storage for (a) 0 day and (b) 90 days, respectively.

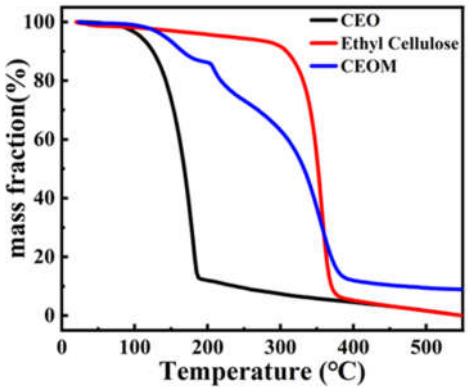


Figure 5. TGA curves of CEO, ethyl cellulose and CEOM.

*Single factor experiment*

*Wall material mass fraction*

The relationship between the concentration of ethyl cellulose and both encapsulation efficiency and yield rate showed in Figure 6a. As the mass fraction of ethyl cellulose rises, there is a noticeable enhancement in encapsulation efficiency and an upward trend in yield rate. When the wall material mass fraction is at 3%, the yield rate hits a maximum of 87%, and at 4%, the encapsulation efficiency reaches its highest point of 76%. However, beyond 3%, elevating the ethyl cellulose content results in a dramatic decline in yield rate. Insufficient amounts of ethyl cellulose lead to incomplete encapsulation, resulting in lower efficiency and yield. Conversely, higher concentrations enable increased coating of the core material, gradually improving encapsulation efficiency and yield rate. However, surpassing the optimum concentration leads to the formation of empty microcapsules, consequently reducing both efficiency and yield rate. In conclusion, 3% is the optimal wall material mass fraction.

*Core wall ratio*

Figure 6b illustrates the impact of the core wall ratio on the encapsulation efficiency and yield rate. As the core wall ratio decreases, there is an initial rise followed by stabilization in microcapsule encapsulation, while the production rate initially increases and then decreases. This pattern can be elucidated as follows: a higher core wall ratio results in a more significant proportion of CEO in the core material and decreased presence of ethyl cellulose in the wall material. Consequently, some CEOs remain unencapsulated, resulting in lower encapsulation and yield rates. A decrease in the core wall ratio reduces the proportion of clove essential oil, allowing more efficient encapsulation within the ethyl cellulose, thereby enhancing the encapsulation and yield rates. Once the maximum encapsulation rate 67% is achieved, further reduction in the core wall ratio maintains a relatively constant encapsulation rate. However, excessive ethyl cellulose at this stage leads to an increase in empty CEOM, thereby reducing the yield rate.

*Mass fraction of emulsifier*

The impact of the mass fraction of emulsifier on both the encapsulation efficiency and yield rate are demonstrated in Figure 6c. As the emulsifier mass fraction rises, there is an initial upsurge followed by a stabilization in encapsulation efficiency and yield rate. When the emulsifier mass fraction is low, the effectiveness of emulsification diminishes, resulting in poor dispersion of CEO within ethyl cellulose, leads CEO to a propensity for aggregation, consequently causing lower rates of encapsulation and reduced microcapsule yield. However, as the emulsifier mass fraction increases, the emulsification process improves, enhancing CEO dispersion capability and boosting both the encapsulation rate and microcapsule yield. Once the water and oil phases reach complete emulsification, further increases in the emulsifier mass fraction have minimal impact on the emulsification process, maintaining the encapsulation rate and yield of CEOM at a relatively steady level.

*Shear rate*

The correlation between shear rate, microcapsule encapsulation efficiency, and yield rate is depicted in Figure 6d. As the shear rate rises, CEOM's encapsulation efficiency and yield rate initially rise before declining. This pattern is attributed to the inadequate dispersion ability of the reaction system at low shear rates, resulting in an uneven mixture of water and oil phases and, subsequently, low encapsulation and yield rates. As the shear rate increases, the dispersion effect improves, leading to a more uniform blend of water and oil phases, thereby enhancing the encapsulation and yield rates. However, upon reaching peak encapsulation and yield rates at 78% and 89%, respectively, further escalation of the shear rate becomes unfavorable for the deposition of clove essential oil on ethyl cellulose, consequently causing a decrease in encapsulation and yield rates.

*Orthogonal array testing*

Based on the single factor experiment, an orthogonal test was conducted to optimize the encapsulation process, resulting in a more suitable encapsulation procedure determined through range analysis. Table 2 illustrates the intuitive analysis outcomes, with Ki and ki representing the average encapsulation efficiency and yield rate for factor level i within the respective columns. R and r denote the difference between the maximum and minimum mean values of the embedding rate and yield within the column, respectively. When evaluating the encapsulation rate as the benchmark, the order of influence of the four factors was determined to be core wall ratio > mass fraction of wall material > shear rate > emulsifier mass fraction. The most favorable combination identified was A2B2C1D2. Conversely, when yield was considered the primary index, the

influence order of the four factors changed, with the mass fraction of wall material being the most influential, followed by core wall ratio, shear rate, and emulsifier mass fraction. The optimal combination in this scenario was A2B2C3D2.

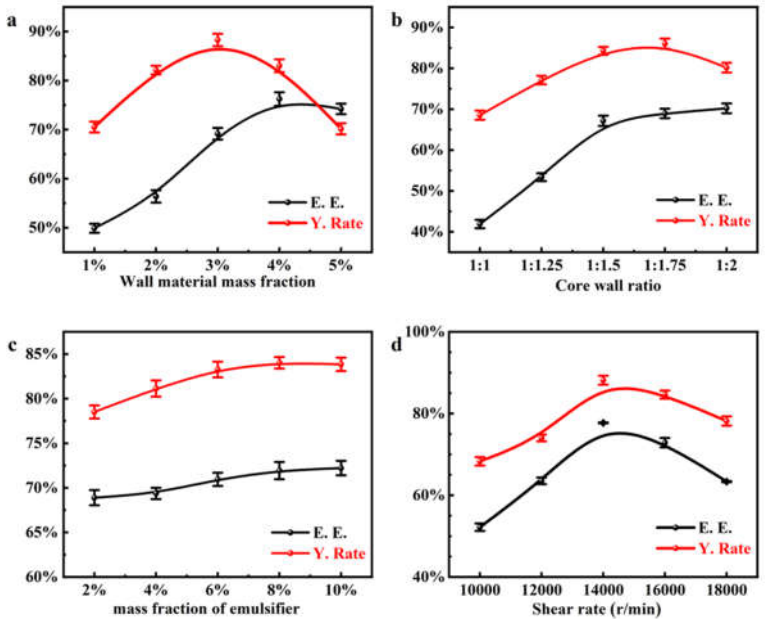


Figure 6. Effects of various factors on the encapsulation efficiency (E.E.) and yield rate (Y. rate) of CEOM. a. Wall material mass fraction. b. Core wall ratio c. Mass fraction of emulsifier. d. Shear rate.

Table 2. Intuitive analysis results of orthogonal tests.

| Serial number | | Factor levels | | | | Encapsulation efficiency (%) | Yield rate (%) |
|---|---|---|---|---|---|---|---|
| | | A | B | C | D | | |
| 1 | | 1 | 1 | 1 | 1 | 51.56 | 71.23 |
| 2 | | 1 | 2 | 2 | 2 | 71.08 | 78.75 |
| 3 | | 1 | 3 | 3 | 3 | 59.50 | 74.17 |
| 4 | | 2 | 1 | 2 | 3 | 57.55 | 83.69 |
| 5 | | 2 | 2 | 3 | 1 | 78.44 | 89.75 |
| 6 | | 2 | 3 | 1 | 2 | 69.28 | 86.48 |
| 7 | | 3 | 1 | 3 | 2 | 55.70 | 78.26 |
| 8 | | 3 | 2 | 1 | 3 | 75.10 | 80.31 |
| 9 | | 3 | 3 | 2 | 1 | 64.43 | 76.56 |
| Encapsulation efficiency | K1 | 182.14 | 164.81 | 195.93 | 194.43 | | |
| | K2 | 205.26 | 224.62 | 193.07 | 196.05 | | |
| | K3 | 195.24 | 193.20 | 193.64 | 192.16 | | |
| | R | 23.12 | 59.81 | 2.863 | 3.89 | | |
| Yield rate | k1 | 224.14 | 233.18 | 238.02 | 237.55 | | |
| | k2 | 259.92 | 248.80 | 238.99 | 243.49 | | |
| | k3 | 235.13 | 237.21 | 242.18 | 238.16 | | |
| | r | 35.78 | 15.63 | 4.17 | 5.96 | | |

Due to potential inaccuracies in the intuitive analysis, the results underwent further analysis via range analysis to identify the key factors influencing the encapsulation effect. These findings are presented in Table 3. The impact of the mass fraction of wall material and core wall ratio on encapsulation and yield was notably significant ($p < 0.01$). In contrast, the influence of the mass fraction of the emulsifier and shear rate was deemed insignificant ($p > 0.05$), aligning with the initial analysis. With a focus on the cost of preparing CEOM, the conditions denoted as A2B2C3D2 were deemed optimal. Specifically, these conditions entail a 3% mass fraction of wall material, a core wall ratio of 1.1:1.5, an 8% mass fraction of emulsifier, and a shear rate of 14000 r/min. Under these parameters, the CEOM exhibited an encapsulation rate of 81.28% and a yield of 90.58%. Based on these parameters, an assessment of the CEOM's sustained-release behavior was conducted.

Table 3. Range analysis results.

| Indicators | Sources of variation | Sum of the squares of deviation | Degrees of freedom | Mean square | F | P |
|---|---|---|---|---|---|---|
| Encapsulation efficiency | Wall material mass fraction | 268.761 | 2 | 134.380 | 84.908 | <0.01 |
| | Core wall ratio | 1790.148 | 2 | 895.074 | 565.549 | <0.01 |
| | Mass fraction of emulsifier | 4.587 | 2 | 2.293 | 1.449 | 0.261 |
| | Shear rate | 7.626 | 2 | 3.813 | 2.409 | 0.118 |
| | Error | 28.488 | 18 | 1.583 | | |
| | Summation | 2099.609 | 26 | | | |
| | $R^2 = 0.980$ | | | | | |
| Yield rate | Wall material mass fraction | 671.740 | 2 | 335.870 | 109.762 | <0.01 |
| | Core wall ratio | 131.605 | 2 | 65.803 | 21.504 | <0.01 |
| | Mass fraction of emulsifier | 9.497 | 2 | 4.749 | 1.552 | 0.239 |
| | Shear rate | 21.428 | 2 | 10.714 | 3.501 | 0.052 |
| | Error | 55.080 | 18 | 3.060 | | |
| | Summation | 889.350 | 26 | | | |
| | $R^2 = 0.911$ | | | | | |

*Sustained release performance of CEOM*

CEOM' slow-release behavior was examined in various package condition simulants: water, 10% ethanol, 50% glycerin, and 3% acetic acid. Figure 7 illustrates that CEO released rapidly in all four mediums, reaching a high cumulative release amount of 95% within 12, 8, 5, and 9 hours, respectively. However, after reaching 95% release, the CEOM exhibited a notable slowdown in their release rate. The initial 36 hours have witnessed a faster release rate, followed by a gradual deceleration and stabilization. Notably, the release rates ranked from high to low were 50% ethanol, 10% ethanol, 3% acetic acid, and water, corresponding to maximum release amounts of 99.32%, 89.21%, 86.16%, and 79.12%, respectively. This pattern was primarily attributed to the higher solubility of the microcapsule's wall and core materials in 50% ethanol than other mediums. These findings underscore the effectiveness of CEOM in efficiently moderating the release rate of CEO, thereby demonstrating their potential in controlled release applications.

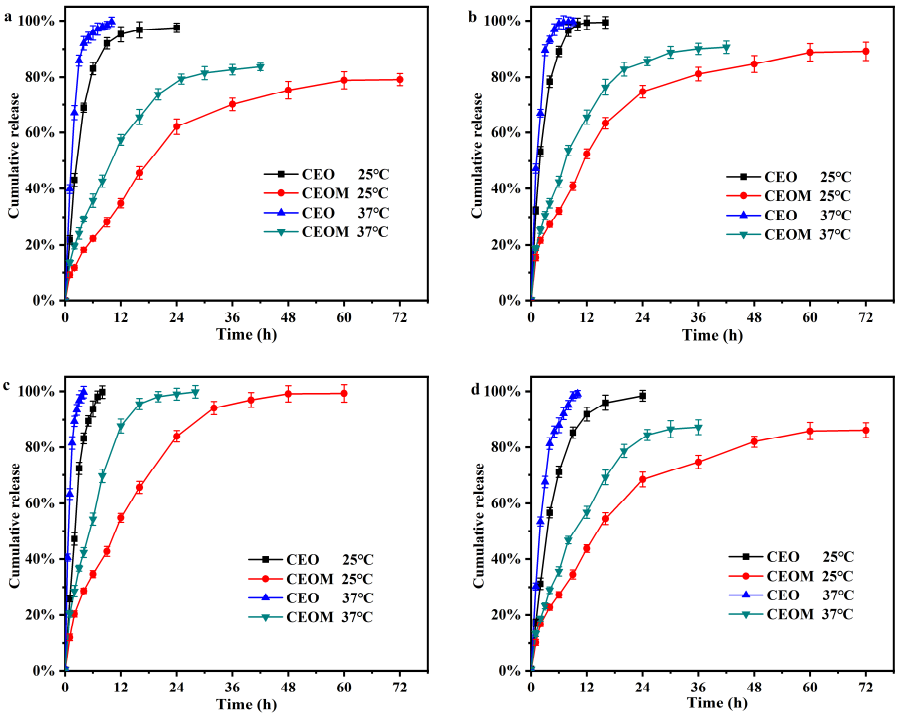


Figure 7. The release profiles of the CEOM at 25 °C and 37 °C in different mediums (a) water, (b) 10% ethanol, (c) 50% glycerin and (d) 3% acetic acid.

At 37 °C, the CEOMs exhibited a quicker release rate across the four media than at 25 °C. The time taken for CEO to reach 95% cumulative release was approximately 6, 4.5, 2.8, and 7.5 hours, respectively. This acceleration at 37 °C primarily stemmed from the increased mobility of both CEO and the CEOM, enhancing their diffusion speed and subsequently expediting the release rate. Nevertheless, the release CEOM remained slower than CEO. These findings emphasize the efficacy of CEOM in effectively decelerating the release rate of CEO at both 25 °C and 37 °C, thereby facilitating controlled release in food packages.

## CONCLUSIONS

The study aimed to optimise CEOM preparation parameters, since EO contained package currently represents an essential alternative to plastics in the frame of the circular economy. CEO was packed using ethyl cellulose, showing acceptable stability and antimicrobial potential [9, 10]. The optimised conditions are as follows: wall mass fraction of 3%, core-wall ratio of 1.1:1.5, emulsifier mass fraction of 8% and shear rate of 14000 r/min. At this condition, the encapsulation efficiency is 81.28%, the yield rate is 90.58%. Meanwhile, CEOM demonstrated reliable sustained-release performance in all four mediums at both 25 °C and 37 °C, effectively extending the antibacterial duration of CEO. In short, CEOM packaging is the potential candidate to substitute the traditional polyethene used for food packaging, where CEOM realise the slow release of CEO. More exhaustive studies for CEOM application in perishable foods, such as

fruitcakes, buns, cookies and cupcakes, and sensory evaluation will be planned in our future works.

## ACKNOWLEDGEMENT

This research received no external funding.

## REFERENCES

1. Araújo Couto, H.G.S.D.; Blank, A.F.; Oliveira e Silva, A.M.d.; Nogueira, P.C.d.L.; Arrigoni-Blank, M.d.F.; Nizio, D.A.d.C.; Pinto, J.A.d.O. Essential oils of basil chemotypes: Major compounds, binary mixtures, and antioxidant activity. *Food Chem.* **2019**, 293, 446-454.
2. Arasu, M.V.; Viayaraghavan, P.; Ilavenil, S.; Al-Dhabi, N.A.; Choi, K.C. Essential oil of four medicinal plants and protective properties in plum fruits against the spoilage bacteria and fungi. *Ind. Crops Prod.* **2019**, 133, 54-62.
3. Reyes-Jurado, F.; Bárcena-Massberg, Z.; Ramírez-Corona, N.; López-Malo, A.; Palou, E. Fungal inactivation on Mexican corn tortillas by means of thyme essential oil in vapor-phase. *Curr Res Food Sci.* **2022**, 5, 629-633.
4. Achar, P.N.; Quyen, P.; Adukwu, E.C.; Sharma, A.; Msimanga, H.Z.; Nagaraja, H.; Sreenivasa, M.Y. Investigation of the Antifungal and Anti-Aflatoxigenic Potential of Plant-Based Essential Oils against Aspergillus flavus in Peanuts. *J. Fungi.* **2020**, 6, 383.
5. Pandey, V.K.; Srivastava, S.; Singh, R.; Dar, A.H.; Dash, K.K. Effects of clove essential oil (*Caryophyllus aromaticus* L.) nanoemulsion incorporated edible coating on shelf-life of fresh cut apple pieces. *J. Agric. Food Res.* **2023**, 14, 100791.
6. Guo, J.; Li, P.; Kong, L.; Xu, B. Microencapsulation of curcumin by spray drying and freeze drying. *LWT Food Sci. Technol.* **2020**, 132, 109892.
7. Jiang, A.; Cai, Y.; Yang, Y.; Wang, H.; She, Z.; Xu, C.; Tai, Z. Temperature-regulated microcapsules containing lavender essential oil are effective natural insecticide against Sitophilus granaries. *Ind. Crops Prod.* **2023**, 203, 117186.
8. Zhang, L.; Zhang, M.; Ju, R.; Bhandari, B.; Liu, K. Antibacterial mechanisms of star anise essential oil microcapsules encapsulated by rice protein-depolymerized pectin electrostatic complexation and its application in crab meatballs. *Int. J. Food. Microbiol.* **2023**, 384, 109963.
9. Wang, H.; Dong, Y.; Qiu, W.; Chen, C.; Xie, J. Development of slow release antibacterial polylactic acid bilayer active film with different distributions of clove essential oil and its application for snakehead (Channa argus) preservation. *Food Cont.* **2024**, 162, 110473,
10. Milagres de Almeida, J.; Crippa, B.L.; Martins Alencar de Souza, V.V.; Perez Alonso, V.P.; da Motta Santos Júnior, E.; Siqueira Franco Picone, C.; Prata, A.S.; Cirone Silva, N.C. Antimicrobial action of Oregano, Thyme, Clove, Cinnamon and Black pepper essential oils free and encapsulated against foodborne pathogens. *Food Cont.* **2023**, 144, 109356.
11. Hedayati, S.; Tarahi, M.; Azizi, R.; Baeghbali, V.; Ansarifar, E.; Hashempur, M.H. Encapsulation of mint essential oil: Techniques and applications. *Adv. Colloid Interface Sci.* **2023**, 321, 103023.
12. Ding, X.; Zhao, L.; Khan, I.M.; Yue, L.; Zhang, Y.; Wang, Z. Emerging chitosan grafted essential oil components: A review on synthesis, characterization, and potential application. *Carbohydr. Polym.* **2022**, 297, 120011.
13. Yang, Y.-h.; Li, X.-z.; Zhang, S. Preparation methods and release kinetics of Litsea cubeba essential oil microcapsules. *RSC Adv.* **2018**, 8, 29980-29987.
14. Asghari-Varzaneh, E.; Shahedi, M.; Shekarchizadeh, H. Iron microencapsulation in gum tragacanth using solvent evaporation method. *Int. J. Biol.Macromol* **2017**, 103, 640-647.

15. van der Kooij, R.S.; Steendam, R.; Frijlink, H.W.; Hinrichs, W.L.J. An overview of the production methods for core–shell microspheres for parenteral controlled drug delivery. *Eur J. Pharm. Biopharm.* **2022**, 170, 24-42.
16. Kong, P.; Abe, J.P.; Enomae, T. Preparation of Antimicrobial 6-cyclodextrin Microcapsules containing a Mixture of Three Essential Oils as an Eco-friendly Additive for Active Food Packaging Paper. *JAP TAPPI J.* **2022**, 76, 656-662.
17. Karimzad Ghavidel, A.; Zadshakoyan, M.; Arjmand, M.; Kiani, G. A novel electro-mechanical technique for efficient dispersion of carbon nanotubes in liquid media. *Int. J. Mech. Sci.* **2021**, 207, 106633.
18. Kong, P.; Abe, J.P.; Masuo, S.; Enomae, T. Preparation and characterization of tea tree oil-β-cyclodextrin microcapsules with super-high encapsulation efficiency. *J. Bioresource Bioprod.* **2023**, 8, 224-234.
19. Mehran, M.; Masoum, S.; Memarzadeh, M. Microencapsulation of Mentha spicata essential oil by spray drying: Optimization, characterization, release kinetics of essential oil from microcapsules in food models. *Ind. Crops Prod.* **2020**, 154, 112694.
20. Tarhan, İ.; Bakır, M.R.; Kalkan, O.; Yöntem, M.; Kara, H. Rapid determination of adulteration of clove essential oil with benzyl alcohol and ethyl acetate: Towards quality control analysis by FTIR with chemometrics. *Vib. Spectros.* **2022**, 118, 103339.
21. Venugopal, G.; Lakshmipathy, R.; Sarada N.C. Preparation and Characterization of Cefditoren pivoxil-loaded liposomes for controlled in vitro and in vivo drug release. *Int. J. Nanomed.* **2015**, 10, 149-157.